ACADEMIC PRESS

Available online at www.sciencedirect.com

SCIENCE DIRECT®

Journal of Computational Physics 184 (2003) 321–337

JOURNAL OF COMPUTATIONAL PHYSICS

www.elsevier.com/locate/jcp

On the computation of a very large number of eigenvalues for selfadjoint elliptic operators by means of multigrid methods

Vincent Heuveline

Institute of Applied Mathematics, Numerical Analysis group IWR, University of Heidelberg, INF 293/294, D-69120 Heidelberg, Germany

Received 6 November 2001; accepted 22 October 2002

Abstract

Recent results in the study of quantum manifestations in classical chaos raise the problem of computing a very large number of eigenvalues of selfadjoint elliptic operators. The standard numerical methods for large eigenvalue problems cover the range of applications where a few of the leading eigenvalues are needed. They are not appropriate and generally fail to solve problems involving a number of eigenvalues exceeding a few hundreds. Further, the accurate computation of a large number of eigenvalues leads to much larger problem dimension in comparison with the usual case dealing with only a few eigenvalues. A new method is presented which combines multigrid techniques with the Lanczos process. The resulting scheme requires $O(mn)$ arithmetic operations and $O(n)$ storage requirement, where n is the number of unknowns and m, the number of needed eigenvalues. The discretization of the considered differential operators is realized by means of p-finite elements and is applicable on general geometries. Numerical experiments validate the proposed approach and demonstrate that it allows to tackle problems considered to be beyond the range of standard iterative methods, at least on current workstations. The ability to compute more than 9000 eigenvalues of an operator of dimension exceeding 8 million on a PC shows the potential of this method. Practical applications are found, e.g. in the numerical simulation of quantum billiards.

Keywords: Eigenvalue problems; Elliptic operators; p-Finite element method; Multigrid method; Lanczos method; Quantum billiards

1. Introduction

In the last decades, the issue of computing part of the spectrum of large matrices has been the object of intensive research activities. Especially the increased need for solving large eigenvalue problems in many scientific and engineering applications have triggered a remarkable shift toward new and efficient iterative methods (see e.g. [38] and references therein). Usually, the number of needed eigenvalues does not exceed a few hundred. In that context, special methods essentially based on *blocking* and *deflation* techniques have been developed in order to be able to compute simultaneously or iteratively the different needed eigenvalues.

E-mail address: vincent.heuveline@iwr.uni-heidelberg.de.

0021-9991/02/$ - see front matter
PII: S0021-9991(02)00043-8

However, recent developments in the study of quantum manifestation of chaos, raise in the foreground the problem of computing a very large number of eigenvalues, usually several thousand (see e.g. [1,15,19]). One is interested in the distribution of the spectrum in order to be able to extract valuable information through statistical analysis of the eigenvalue sequence (see [1] for more details). This problem constitutes a challenging numerical task for mainly two reasons: The accurate determination of a large number of eigenvalues with regard to their discretization errors relies on much finer discretization of the considered operator than for the computation of a few eigenvalues. This leads to very large eigenvalue problems for which the computation of even a single eigenvalue may become extremely cumbersome if possible at all, considering classical iterative projection methods on conventional workstations. Further, it is well known that the standard *blocking* and *deflation* techniques have limitations with regard to the number of computed eigenvalues mainly due to memory requirement constraints as well as numerical instabilities connected to rounding errors.

Despite increasing demand especially in the study of chaos in quantum mechanics, the development of efficient methods for computing a very large number of eigenvalues has been paid little attention to. The goal of this paper is to fill this gap for the case of elliptic selfadjoint operators.

The proposed approach does not make any assumption on the considered geometry and does not intend to take advantage of parallel high-performance computer facilities. In fact, it allows to tackle such problems on the most common workstations. It relies on three main ingredients. The most expensive part of the proposed algorithm is the resolution at each step of a linear system by means of a multigrid method. The CPU costs and memory requirements scale linearly with the number of unknowns which allows one to solve very efficiently large problems (several millions of unknowns) on a common workstation. The proposed approach takes advantage of the so-called *Lanczos phenomenon* [10] which ensures that at some step despite rounding errors, every distinct eigenvalue of the considered discrete problem is an eigenvalue of the tridiagonal operator generated by the Lanczos process. Furthermore , the filtering procedure proposed by the key work of Cullum and Willoughby [11] has been considered in order to eliminate the spurious eigenvalues.

The outline of the remainder of this paper is as follows. In Section 2, we establish notations and formulate the generalized eigenvalue problem resulting from a finite element discretization. Special emphasis is put on the dependency of the discretization error with the real part of the considered eigenvalues. In Section 3, we describe the newly developed method. In Section 4, numerical experiments for the model problem of the Poisson equation on various geometries are presented.

2. Finite element discretization

Let L be a selfadjoint uniformly elliptic differential operator on a bounded domain $\Omega \subset \mathbb{R}^d$. The classical formulation of the eigenvalue problem for this operator reads

$$Lu = \lambda u \quad \text{in} \quad \Omega, \quad B_j u = 0 \quad \text{on} \quad \partial\Omega \quad (j = 1, \ldots, q), \tag{2.1}$$

where $\{B_j\}_{j=1,\ldots,q}$ are boundary operators. This classical representation can be replaced by the following variational formulation:

$$\text{Find} \quad \lambda \in \mathbb{C}, 0 \neq u \in V \quad \text{with} \quad a(u,v) = \lambda(u,v) \quad \forall v \in V, \tag{2.2}$$

where $(u,v) = \int_\Omega u \cdot v \, dx$ is the $L^2(\Omega)$ scalar product, V is an appropriate Sobolev space, $V \subset L^2(\Omega) \subset V'$ build a Gelfand triple and $a : V \times V \to \mathbb{R}$ is a suitable sesquilinear form which may be assumed to be V-coercive (see Gårding theorem e.g. [44, p. 175]).

Let $V_h \subset V$ be a finite element space, where $h \in \mathbb{R}_+$ is the discretization parameter. The finite element discretization of (2.2) reads (see e.g. [21, chapter 11] for more details):

$$\text{Find } \lambda_h \in \mathbb{R}, 0 \neq u_h \in V_h : \quad a(u_h, v) = \lambda_h(u_h, v) \qquad \forall v \in V_h. \tag{2.3}$$

In algebraic notation (2.3) reads as the following generalized eigenvalue problems

$$\mathbf{L}_h u_h = \lambda_h \mathbf{M}_h u_h. \tag{2.4}$$

$\mathbf{L}_h$ (resp. $\mathbf{M}_h$) represents the *stiffness* (resp. *mass*) matrix. Both are in our context symmetric and positive definite. In the following, the subscript h (resp. l) refers to the mesh size (resp. the refinement level) of the triangulation of Ω. In order to simplify the notations, these subscripts will be omitted if the discrete nature of the considered space, operator or function is obvious. In the remainder of this paper, $\langle ., . \rangle$ (resp. $\langle ., . \rangle_{\mathbf{M}_h}$) describes the Euclidean scalar product (resp. the scalar product induced by the mass matrix $\mathbf{M}_h$) and $\{(\lambda_s; u_s)\}_{s=1,n}$ (resp. $\{(\lambda_{h,s}; u_{h,s})\}_{s=1,n}$) represents the eigenpairs of (2.2) (resp. (2.3)).

Since L is selfadjoint, the eigenfunctions of (2.2) and (2.3), respectively, can be chosen $L_2(\Omega)$ orthogonal the corresponding eigenvalues are real. Furthermore, the eigenfunctions are the stationary points u_s of the Rayleigh quotient

$$\mathscr{R}(v) := \frac{a(v, v)}{(v, v)}, \tag{2.5}$$

and the corresponding eigenvalues are $\lambda_s = \mathscr{R}(u_s)$. This characterization allows to derive the following upper bounds for the discretization error of the computed eigenvalues (see [41]):

Lemma 1. *Let L be an elliptic selfadjoint operator of order $2r$ which is H^k-regular, where $k - 1$ is the polynomial degree of the finite element shape functions. Under the usual assumptions of the finite element discretization (see e.g. [8]) the eigenvalue error satisfies*:

$$\lambda_{h,s} - \lambda_s \leqslant C \lambda_s^{k/r} h^{2(k-r)}. \tag{2.6}$$

For the more general non-selfadjoint case, more involved techniques allow to derive similar results [4,7,31].

It is important to notice that the error bound (2.6) indicates that for a given triangulation the accuracy of the higher eigenvalues deteriorates with the coefficient $\lambda_s^{k/r}$. This behavior is observed in practice and shown in Fig. 2. The accurate computation of a large number of eigenvalues leads therefore, to much finer discretizations compared with the classical case where only a few eigenvalues are needed. This is illustrated in Table 1 for different finite element discretization orders. It has to be noticed, in that context, that an economical discretization, measured in the number of unknowns, results from the trade-off between the order of the discretization k and the discretization refinement level h [39]. This issue is inherently problem dependent: firstly, it greatly depends on the number of needed eigenvalues and their distribution. Secondly, a valid resolution of the considered geometry may rely on h-refinement.

Remark 1. On principle, the techniques presented in this paper could be derived in the context of the boundary element method (BEM). However, a sparsity pattern similar to the matrices $\mathbf{L}_h$ and $\mathbf{M}_h$, respectively, (see Eq. (2.4)) obtained by means of a finite element method discretization cannot be obtained in such a straightforward way considering the boundary element method and involves additional technicalities (see e.g. [22] and references therein). The treatment of geometries with corners which is of importance in our context (see Section 4) imposes also a special treatment in the discretization step. Further, the boundary element method is not well suited for differential operators with variable coefficients. This

Table 1
Number of converged eigenvalues N_λ and number of validated converged eigenvalues N_λ^{val} (see Section 3.3) depending on the discretization

# Dofs	Q_1		Q_2		Q_4		Q_8	
	N_λ	N_λ^{val}	N_λ	N_λ^{val}	N_λ	N_λ^{val}	N_λ	N_λ^{val}
4225	48	**0**	154	**0**	240	**0**	513	**0**
16641	80	**22**	310	**72**	500	**112**	823	**160**
66049	157	**48**	613	**148**	1200	**240**	–	–
263169	325	**80**	1230	**324**	2390	**500**	–	–
~1 Mi.	657	**157**	2423	**613**	–	–	–	–
~4 Mi.	1284	**323**	4915	**1228**	–	–	–	–
~8 Mi.	2458	**657**	9256	**2423**	–	–	–	–

Convergence is assumed for a relative discretization error below $tol = 1 \times 10^{-3}$.
Empty entries corresponds to an exceed of the memory capacity.

case encompasses however the important class of problem where the considered geometries have non-homogeneous material properties. For these reasons this method has not been further considered in this paper.

3. Multigrid method and Lanczos tridiagonalization

The goal of this section is to describe the proposed solution process. It is based on the interplay between multigrid techniques for linear systems and the symmetric Lanczos algorithm. Furthermore, the issue of the validation of the computed eigenvalues, which is essential in our context, is addressed.

3.1. Lanczos tridiagonalization and spectral transformation

For simplicity, we first consider the standard discrete eigenvalue problem

$$\mathbf{C}_h u_h = \lambda_h u_h, \tag{3.7}$$

where $\mathbf{C}_h \in \mathbb{R}^{n\times n}$ is symmetric and $u_h \in \mathbb{R}^n$. The standard symmetric Lanczos method [27] can be interpreted as a *Galerkin* projection method with respect to the Euclidean inner product on the Krylov subspaces

$$\mathscr{K}_m(\mathbf{C}_h, v_1) := \mathrm{span}\{v_1, \mathbf{C}_h v_1, \ldots, \mathbf{C}_h^{m-1} v_1\},$$

where $v_1 \in \mathbb{R}^n$. This is equivalent to the following problem:
For $s \in [1, m]$, find $\tilde{\boldsymbol{u}}_{h,s} \in \mathscr{K}_m(\mathbf{C}_h, v_1)$ and $\tilde{\lambda}_{h,s} \in \mathbb{R}$ such that

$$\tilde{\lambda}_{h,s} = \min_{\substack{S\subset\mathscr{K}_m(\mathbf{C}_h,v_1)\\ \dim(S)=m-s+1}} \max_{u\in S} \frac{\langle \mathbf{C}_h u, u\rangle}{\langle u, u\rangle}, \tag{3.8}$$

$$(\mathbf{C}_h - \tilde{\lambda}_{h,s} I)\tilde{\boldsymbol{u}}_{h,s} \perp \mathscr{K}_m(\mathbf{C}_h, v_1). \tag{3.9}$$

Let $V_m = [v_1, \ldots, v_m]$ be an orthonormal basis of $\mathscr{K}_m(\mathbf{C}_h, v_1)$. Condition (3.8) obviously defines the subset $\{\tilde{\lambda}_{h,s}\}_{s=1,\ldots,m}$ as the set of eigenvalues of the symmetric matrix

$$\mathbf{H}_m := V_m^{\mathrm{T}} \mathbf{C}_h V_m. \tag{3.10}$$

Notice that due to the intrinsic structure of Krylov subspaces the matrix H_m is of Hessenberg form. Since $\mathbf{C}_h$ is assumed to be symmetric, $\mathbf{H}_m$ is also symmetric and has therefore, the following symmetric tridiagonal form:

$$\mathbf{H}_m = \begin{bmatrix} \alpha_1 & \beta_2 & & & & \\ \beta_2 & \alpha_2 & \beta_3 & & & \\ & \beta_3 & \cdot & \cdot & & \\ & & \cdot & \cdot & \cdot & \\ & & & \cdot & \cdot & \beta_m \\ & & & & \beta_m & \alpha_m \end{bmatrix}. \tag{3.11}$$

The Lanczos algorithm provides an efficient set-up to compute the coefficients of the matrix $\mathbf{H}_m$. It relies on the following relation which for Krylov subspaces holds by construction:

$$\mathbf{C}_h V_m = V_m \mathbf{H}_m + w_m e_m^{\mathrm{T}}, \tag{3.12}$$

where $\langle w_m, v_i \rangle = 0 \ \forall i \in [1, m]$ and $e_m = (0, \ldots, 0, 1)^{\mathrm{T}}$. The expression (3.11) of $\mathbf{H}_m$ applied to (3.12) leads to the well-known three-term recurrence relation

$$\beta_{j+1} v_{j+1} = \mathbf{C}_h v_j - \alpha_j v_j - \beta_{j-1} v_{j-1} \quad j \geqslant 2, \tag{3.13}$$

from which the Lanczos Algorithm 1 may be directly derived. To improve the numerical stability we consider the modified Gram–Schmidt variant of the Lanczos algorithm [32,33]. In exact arithmetic, the vectors $\{v_i\}_{i=1,\ldots,m}$ are orthogonal and for $m = n$, $\mathbf{H}_m$ is a symmetric tridiagonal matrix congruent to $\mathbf{C}_h$. In practice however, severe loss of orthogonality due to rounding errors is encountered and leads to the existence of *spurious eigenvalues*. Their treatment is a crucial issue in our context and is postponed to Section 3.3.

Algorithm 1 (*Symmetric Lanczos algorithm*)

Choose v_1 such that $||v_1|| = 1$ and $\langle v_1, u_{h,s} \rangle \neq 0$ for $s \in [1, m]$
Set $\beta_1 = 0$, $v_0 = 0$
for $i = 1$ **to** m **do**
  $w_i := \mathbf{C}_h v_i - \beta_i v_{i-1}$
  $\alpha_i := \langle w_i, v_i \rangle$; $w_i := w_i - \alpha_i v_i$
  $\beta_{i+1} := ||v_i||$; $v_{i+1} := w_i / \beta_{i+1}$
end for

The original problem (2.4) is now embedded in the previously derived framework. The relevant eigenvalues of problem (2.4) are in the lower part of the spectrum. In order to first gain convergence against these eigenvalues we therefore, consider a standard spectral transformation leading to the following formulation (see e.g. [13,30]):

$$[(\mathbf{L}_h - \sigma \mathbf{M}_h)^{-1} \mathbf{M}_h] u_h = \frac{1}{\lambda_h - \sigma} u_h. \tag{3.14}$$

The operator $(\mathbf{L}_h - \sigma \mathbf{M}_h)^{-1} \mathbf{M}_h$ is indeed non-symmetric but is selfadjoint with regard to the $\langle ., . \rangle_{\mathbf{M}_h}$ inner product. The Lanczos method remains therefore, valid provided that we replace the Euclidean inner product by $\langle ., . \rangle_{\mathbf{M}_h}$, the inner-product associated to $L_2(\Omega_h)$. This leads to Algorithm 2 which is the core procedure of our approach.

Algorithm 2 (*Spectral transformation Lanczos algorithm*)
Choose v_1 such that $||v_1||_{\mathbf{M}_h} = 1$ and $\langle v_1, u_{h,s}\rangle_{\mathbf{M}_h} \neq 0$ for $s \in [1, m]$
Set $\beta_1 = 0$, $v_0 = 0$
for $i = 1$ **to** m **do**
$w_i := (\mathbf{L}_h - \sigma\mathbf{M}_h)^{-1}\mathbf{M}_h v_i - \beta_i v_{i-1}$
$\alpha_i := \langle w_i, v_i\rangle_{\mathbf{M}_h}$; $w_i := w_i - \alpha_i v_i$
$\beta_{i+1} := ||v_i||_{\mathbf{M}_h}$; $v_{i+1} := w_i/\beta_{i+1}$
end for

The resolution of the linear system in Algorithm 2 is by far the most CPU time consuming part and is solved by means of multigrid techniques (see Section 3.2).

The computation of the eigenvalues of the matrix $\mathbf{H}_m$ is done by means of the Lapack routine DSTERF, which implements a variant due to Pal, Walker and Kahan of the QR method for symmetric tridiagonal matrices [2]. The related CPU time (resp. memory) requirements behave asymptotically like $O(m^2)$ (resp. $O(m)$) and, since $m \ll n$, are negligible in the overall solution process.

Approaches based on rational Krylov subspaces [36], which allow one to adapt the shift term σ along the Lanczos iterations without a complete restart have been discarded. On the one hand, the operator $(\mathbf{L}_h - \sigma\mathbf{M}_h)$ may become indefinite, which may result in severe slow down of the convergence rate of the multigrid iterations. On the other hand, these techniques involve matrices $\mathbf{H}_m$, which are either Hermitian [28] or of Hessenberg form [36] and which are generally non-tridiagonal i.e., with memory requirements growing like $O(m^2)$. In practice this growth may become intractable when a large number n_λ of eigenvalues is needed since $m \approx 2n_\lambda$.

Since the eigenvectors are not needed in our context, we do not make use of the relation (3.9). Therefore, beside the multigrid data structure (see Section 3.2) and the mass matrix $\mathbf{M}_h$, the memory requirements are limited to four vectors. It scales asymptotically with the linear factor $O(n)$, where n is the number of degrees of freedom of the discretization. This property is essential. It allows one with reasonable hardware resources to handle the very large eigenvalue problems needed to gain a valuable discretization error for a large amount of eigenvalues (see the a priori error approximation (2.6)).

3.2. Multigrid solver

The considered variant of the Lanczos algorithm (see Algorithm 2) involves the resolution of the linear system

$$\mathbf{A}_h w = f_h, \tag{3.15}$$

where $\mathbf{A}_h := \mathbf{L}_h - \sigma\mathbf{M}_h$ and $f_h := \mathbf{M}_h v_i$. Since we assume L to be a uniformly elliptic differential operator (see expression (2.1)), the resolution of the linear problem (3.15) falls in the classical framework of multigrid theory (see e.g. [20,43]). Over the last decades, the development of multigrid techniques has been the object of flourishing research activities resulting in a multitude of publications. The underlying algorithmic, although it has become a well-known standard in the meanwhile, is still considered quite involving. We therefore, restrict this section to a brief outline of the considered method putting special emphasis on the specific aspects in our context. For more details, the reader should refer to classical literature such as [20,43].

Multigrid methods, in their classical setup, rely on the existence of a nested triangulation hierarchy $\{\mathscr{T}_{h_l}\}_{l=1,\ldots,l_{\max}}$ with $\mathscr{T}_{h_l} \subset \mathscr{T}_{h_{l+1}}$ which describes the original domain Ω. Replacing h by h_l in (2.3) and (2.4) allows one to define the corresponding discrete eigenvalue problems and therefore, the associated linear systems (3.15) on that triangulation hierarchy. For elliptic operators, multigrid techniques are based on the ability to successively filter on the grid hierarchy the high frequency modes of the error by means of the so

called smoothers (see e.g. [20, chapter 3]). The resulting scheme depicted in Algorithm 3 in its most standard setting has convergence rates which are independent of the discretization level l. The operator $\mathbf{P}_{l-1}^{l}$ describes an adequate prolongation operator between level $l-1$ and level l (see e.g. [20] for more details). This leads for Algorithm 3 to a complexity of $O(n \log n)$ arithmetic operations and $O(n)$ storage requirements.

Algorithm 3 ($MG(l, u, f)$)

if $l = 0$ **then**
  $u := \mathbf{A}_{h_1}^{-1} f$; Exact solution on coarse grid
else
  $\tilde{u} := \mathscr{S}^{(\nu_1)}(u, f)$; $d := \mathbf{A}_{h_l}\tilde{u} - f$; Presmoother/Restriction of residual
 for $j = 1$ **to** γ **do**
   $v = 0$; MG(l–1, v, d)
 end for
  $u := \tilde{u} - \mathbf{P}_{l-1}^{l} v$; $u := \mathscr{S}^{(\nu_2)}(u, f)$; Coarse grid correction/Postsmoother
end if

In order to solve the linear system (3.15), we consider the full multigrid method (FMG) which allows to reduce the number of arithmetic operations to $O(n)$ by embedding Algorithm 3 in a *nested iteration* in the sense of Algorithm 4. The right hand sides f_{h_l} for $l \in [1, l_{\max} - 1]$, where $h_{l_{\max}} := h$ are defined as the L_2-projection of f_h on V_{h_l} i.e.,

$$(f_{h_l}, v) = (f_h, v) \quad \forall v \in V_{h_l}.$$

In the numerical experiments presented in Section 4, we consider V-cycles i.e., $\gamma = 1$ in Algorithm 3 and two pre- and post-smoothing steps by means of the Gauss–Seidel method i.e., $\nu_1 = \nu_2 = 2$.

In addition it is important to notice that in order to gain optimal smoothing properties (see e.g. [20,24]), the shift σ is chosen such that $\mathbf{A}_h$ is positive definite. For the Laplace operator we therefore, impose $\sigma = 0$.

Algorithm 4 (*Nested iteration*)

Choose $w_{start} \in V_{h_1}$;
for $l = 1$ **to** l_{max} **do**
  If $(l > 1)$ $w_{start} = I_{h_l}^{h_{l+1}} w_{h_l}$; (Prolongation)
  Solve $\mathbf{A}_{h_l} w_{h_l} = f_{h_l}$ by means of $\mathrm{MG}(l, w_{start}, f_{h_l})$; (Algorithm 3)
end for

3.3. Assessment of the computed eigenvalues

The previously proposed numerical scheme allows one to calculate very large sequences of approximated eigenvalues. In practice, due to rounding errors, a number of approximated eigenvalues even exceeding the number of degrees of freedom can be found by discarding the theoretical limitation $m \leqslant n$ leading to a breakdown in Algorithm 2. This somewhat incongruous situation emphasizes the necessity of an a posteriori validation mechanism in order to separate *true* approximated eigenvalues from discretization artefacts and spurious eigenvalues. The treatment of this issue is presented in this section and beside the use of multigrid techniques in the context of the Lanczos iteration, is a cornerstone of the proposed approach.

The overall solution process can be interpreted as a nested Galerkin approximation scheme including two levels: the discretization of the differential operator and the iterative resolution of the discrete eigenvalue problem by means of the Lanczos method.

The error due to the finite element discretization is controlled by means of the a priori error estimation (2.6). The eigenvalue problem (2.4) is solved on a hierarchy of refined discretizations until the predicted asymptotic convergence behavior of the needed eigenvalues is detected. This is done by means of an adequate pairing between the computed eigenvalues on successive refinement levels. This procedure is combined with extrapolation techniques similar to those proposed by Blum et al. [6]. For the converged eigenvalues, they allow one to gain an upper bound for the error discretization as well as an increased accuracy on the last discretization level.

The validation of the computed eigenvalues in the Lanczos Algorithm 2 is much more tedious. Indeed, the computation of a large number of eigenvalues n_λ relies obviously on a large number of iterations m in the Lanczos procedure 2 since $m \geqslant n_\lambda$. For such large m, rounding errors result in a global loss of orthogonality of the Krylov subspace basis $\{v_i\}_{i=1,m}$ leading to spurious eigenvalues (see e.g. [37]). Several techniques based on *full* or *partial reorthogonalization* of the Lanczos vectors v_i allow to cure this problem. They are mainly based on keeping track either of the whole or part of the the basis $\{v_i\}_{i=1,m}$ or of the converged eigenfunctions (see [37] and references therein). The resulting storage and CPU time requirements would be intractable in our approach. Our approach is based on the astonishing result due to Cullum and Willoughby [11]. They argue that any eigenvalue of $\mathbf{H}_m$ that is pathologically close to eigenvalues of $\hat{\mathbf{H}}_m$ will be spurious, where $\hat{\mathbf{H}}_m$ denotes the symmetric tridiagonal matrix of order $m-1$ such that

$$\begin{cases} \hat{\mathbf{H}}_m(i,i) = \alpha_{i+1} & \text{for } i = 1, m-1, \\ \hat{\mathbf{H}}_m(i,i+1) = \beta_{i+2} & \text{for } i = 1, m-2. \end{cases} \tag{3.16}$$

The practicability and accuracy of this filtering scheme demonstrated in [11] for eigenvalue problems of order at most 5000, are observed in our context of very large eigenvalue problems. The resulting Algorithm 5 allows indeed to sharply differentiate between true and spurious eigenvalues. It should be emphasized that the multiplicities of multiple eigenvalues cannot be computed using this approach. This is by no mean a restriction in our applications where only the eigenvalue distributions are needed.

Algorithm 5 (*Spurious eigenvalue filtering algorithm*)

Label the eigenvalues $\{\tilde{\lambda}_k\}_{k=1,m}$ of $\mathbf{H}_m$ as true eigenvalue
Compute $\hat{\mathbf{H}}_m$ by means of (3.16) and its eigenvalues $\{\hat{\lambda}_k\}_{k=1,m-1}$
for $i = 1$ **to** m **do**
  if $\tilde{\lambda}_i$ is simple **then**
    if there is $k \in [1, m-1]$ such that $\tilde{\lambda}_i - \hat{\lambda}_k < \max(1, \tilde{\lambda}_i) \cdot Tol$ **then**
      Label $\tilde{\lambda}_i$ as spurious eigenvalue
    end if
  end if
end for

The loss of global orthogonality of the Krylov subspace basis results in a matrix $\mathbf{H}_n$ which may not be equivalent to $\mathbf{C}_h$ (see expression (3.10)). Fortunately, it can be observed and partly proved that local orthogonality inherited from the three term recurrence (3.13) numerically suffices because of the so-called *Lanczos phenomenon* (see [10] and references therein): For large enough m (eventually $m > n$), every distinct eigenvalues of $\mathbf{C}_h$ is an eigenvalue of $\mathbf{H}_m$. The argumentation in [10] is based on the equivalence between the Lanczos tridiagonalization procedure and the conjugate gradient method (see [16,26,38]). It takes advantage of the well-known minimization properties of the conjugate gradient method despite rounding errors. In practice, we observe that the convergence of the n_λ discrete eigenvalues is achieved for $m \in [\frac{3}{2}n_\lambda, 2n_\lambda]$.

It is important to notice that the resolution of the linear system in Algorithm 2 must be performed very accurately since it is not included in any defect correction scheme (see [24] and reference therein). In practice, the solution is computed up to machine accuracy. For quantitative results on the convergence rate of the multigrid method for the Laplace operator we refer to Trottenberg et al. [42].

4. Numerical experiments

The development of the proposed method in Section 3 has been initiated by concrete needs in connection with the study of quantum manifestations of classical chaos by means of spectral fluctuation properties of dynamical systems [19]. Although general and applicable to any selfadjoint elliptic problems, our approach is illustrated in this section by problems arising in that extremely challenging area.

The theoretical investigation of two-dimensional Euclidean and Riemannian geometries, so-called billiard, has been the object of intensive research activities over the last few decades (see [19] and references therein). Plain billiards belong to the class of Hamiltonian systems with the lowest degree of freedom in which chaos can occur. The classical billiards, i.e., plane two-dimensional areas in which ideal particles propagate with specular reflection on the walls, have as analogon the quantum billiard, the spectral properties of which are completely described by the stationary Schrödinger equation

$$\Delta\Psi(\vec{r}) = -k^2\Psi(\vec{r}), \tag{4.17}$$

$$\Psi(\vec{r})|_{\delta\Omega} = 0, \tag{4.18}$$

where

$$k = \sqrt{\frac{2m\mathscr{E}}{\hbar^2}}$$

for particle of mass m and energy $\mathscr{E}$. For classical billiards the dynamic of particles can be either regular, chaotic, or mixed depending only on the shape of the boundary. The natural question whether this classification applies for the associated quantum billiard is still an object of intensive research activities. It has been found out that the distribution of the spectrum of the stationary Schrödinger problem (4.17) and (4.18) is the determining factor in this analysis. The pioneering work of Gutzwiller [18] establishes the relationship between the density states of chaotic quantum systems and the periodic orbits of the classical system. Further, it can been shown that the spectral fluctuation properties of the quantum system coincide with those of the ensemble from Random Matrix Theory (RMT), whereas for time reversal invariant systems, the relevant ensemble is the Gaussian orthogonal ensemble (GOE) (see [17] for more details).

These different approaches have in common that they rely on the knowledge of a large number of eigenvalues of the stationary Schrödinger equations (4.17) and (4.18) i.e., of the Laplace operator on the considered Billiard geometries. Great effort has been made to construct microwave resonators which in that context act as analog eigenvalue solver since they allow to determine experimentally a great amount of eigenvalues (see [35] and references therein). These resonators are based on the well-known analogy between the stationary Schrödinger equation for a two dimensional and infinitely deep potential and the stationary Helmholtz equation

$$\Delta\vec{E} = -k^2\vec{E} \tag{4.19}$$

with

$$k = \frac{2\pi f}{c}, \tag{4.20}$$

where f denotes the frequency, c the velocity of light and $\overrightarrow{E}$ the electric field, which vanishes on the boundary. Indeed, in a sufficiently flat cavity, the electric field is perpendicular to the bottom and top surfaces of the billiard i.e.,

$$\overrightarrow{E} = |\overrightarrow{E}|\overrightarrow{e}_z.$$

It has to be noted that experimentally the maximal resolved frequency $f_{\max}$ has to fulfill $f_{\max} \leqslant \frac{c}{2d}$, where d is the height of the billiard.

The method described in Section 3 allows the numerical treatment of the subsequent problem on almost any geometry. The presented results which range from simple and isospectral geometries to to the well-known Bunimovich billiard geometry clearly show the potentiality of this method. All computations have been performed on a Pentium III/700 MHz/2 GB PC. The eigenvalue solver is defined and implemented in a special module of the more general purpose C++ finite element package *HiFlow* [23]. The eigenfunctions plotted to illustrate the complex features appearing on these special geometries have been computed by means of the method presented in [24].

For the p-finite element discretization, we consider shape functions built by tensor product of the integrated Legendre-polynomials

$$\phi_i(x) := \sqrt{\frac{2i-1}{2}} \int_{-1}^{x} L_{i-1}(\xi)\,\mathrm{d}\xi,$$

where $i \geqslant 2$, $\phi(\pm 1) = 0$ and $L_i(\xi)$ describes the Legendre polynomial of degree i (see [3,29] for more details). This choice has the advantage for the special case of the Laplace operator that the degrees of freedom inside each cell fully decouple from each other leading to economical storage requirements for the stiffness matrix as well as efficient smoothing steps in Algorithm 3. This property does not hold for the mass matrix needed in Algorithm 2 for the inner products. As illustrated in Table 1, at equal number of degrees of freedom, the needed storage requirements increases therefore, greatly with the order of discretization.

It has to be noted that assuming a linear distribution of the spectrum $\lambda_s \sim s$ (case of the unit square) and under the minimal constraints on the absolute error $|\lambda_{h,s} - \lambda_s| \leqslant tol$ for $s \in [1, m]$, the a priori estimation (2.6) allows to derive the asymptotic of the needed number of degrees of freedom. For bilinear finite elements, it corresponds to $\mathrm{O}(m^2)$ (resp. $\mathrm{O}(m^3)$) degrees of freedom for two- (resp. three) dimensional geometries. For biquadratic finite elements, these asymptotic behaviors reduce to $\mathrm{O}(m^{3/2})$ (resp. $\mathrm{O}(m^{9/4})$) on the corresponding geometries.

4.1. Validation on simple geometries

The stationary Schrödinger equations (4.17) and (4.18) may be reformulated in the following form considering the framework of Section 2 (see expression (2.1)):

$$-\Delta u = \lambda u \quad \text{in} \quad \Omega, \quad u = 0 \quad \text{on} \quad \partial\Omega. \tag{4.21}$$

In order to validate our approach, we first consider the unit square and the unit disc for which the spectrum may be derived analytically [9]. For $\Omega := [0,1]^2$ the eigenvalues of the Laplace operator are known to be

$$\lambda_{ij} = (i^2 + j^2)\pi^2 \quad i, j, \in \mathbb{N} \setminus \{0\}.$$

For the unit disc $\Omega := \{(x,y) : x^2 + y^2 < 1\}$. The eigenvalues are defined by

$$\lambda_{kj}^{lap} = \mu_{kj}^2, \qquad k = 0,\ 1,\ \ldots, \qquad j = 1,\ 2, \ldots,$$

where μ_{kj} is the jth root of the kth *Besselfunction* of the first kind.

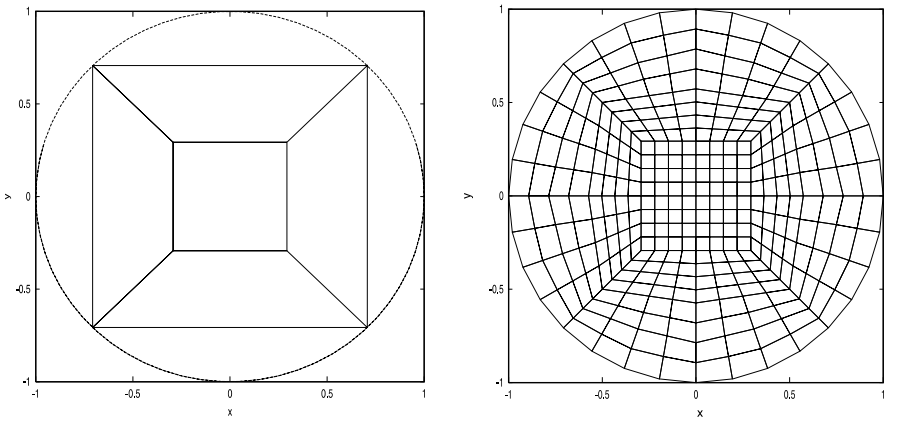

Fig. 1. Start grid (left), third refinement (right) for problem (4.21) on the unit disc.

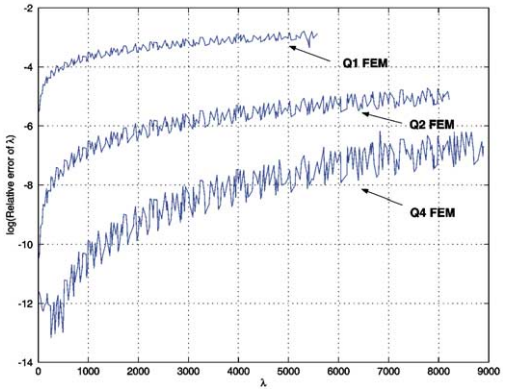

Fig. 2. Relative error discretization of the converged eigenvalues on the unit square for Q_1 (261169 unknowns), Q_2 (261169 unknowns) and Q_4 (66049 unknowns).

The grid hierarchy is obtained by uniform refinement of a start grid, projecting the new nodes on the boundary. For the unit circle, the coarse grid and the third refinement level are plotted on Fig. 1. Fig. 2 shows the behavior of the relative discretization error for Q_1, Q_2, and Q_4 isoparametric finite elements. These results are in good agreement with the a priori error estimation (2.6). They illustrate the expected superiority of the higher order finite elements with regard to the discretization error of the lowest eigenvalues as well as that this gain diminishes for the higher eigenvalues. The asymptotic behavior of Q_2 and Q_4 on Fig. 2 illustrates this phenomenon which results from the larger increase of the term $\lambda_s^{k/r}$ on the right-hand side of expression (2.6) for higher order finite elements.

In practice, it is crucial to be able to validate the eigenvalues a posteriori. Table 1 shows the dependence of the number of converged eigenvalues N_λ on the number of degrees of freedom as well as on the order of the finite element discretization. An eigenvalue is considered to have converged for a relative discretization error below $tol = 1 \times 10^{-3}$. The corresponding number of a posteriori validated eigenvalues by means of the procedure depicted in Section 3.3 is denoted by N_λ^{val}. It determines the number of eigenvalues which can be detected to have converged without the knowledge of the exact

Table 2
Number of converged eigenvalues for the unit circle with Q_2 finite element discretization

# Dofs	5057	20358	81665	327169	~1 Mi.	~4 Mi.	~8 Mi.
N_λ	0	62	184	345	789	1834	4356
N_λ^{val}	**0**	**10**	**31**	**83**	**234**	**734**	**1624**

The notations are similar to Table 1.

Table 3
CPU time distribution for the computation of the 9256 smallest eigenvalues for the unit square with ~8 million unknowns and Q_2 finite elements

		CPU time (s)	CPU time (%)
Multigrid	Smoother	1.7×10^5	42
	Grid transfer	1.3×10^5	32
	Residual	2.8×10^4	7
Lanczos	Inner products	3.2×10^4	8
	Spectrum of H_m	8.2×10^3	2
Miscellaneous		3.7×10^4	9

solution. Despite the theoretical superiority of higher order discretizations, Table 1 clearly shows that they have the main drawback that for a given memory capacity they are restricted to a much smaller discretization hierarchy than their lower order counterpart. Due to their inherent coupling the storage requirements shift indeed from $O(n)$ to $O(n^2)$ for higher order, where n is the number of unknowns. In practice we therefore, consider Q_2 finite elements. Using the same notations, the discretization error history for the unit circle is given in Table 2. Table 3 summarizes the CPU cost distribution related to the computation of the 9256 smallest eigenvalues for the unit square using ~8 million unknowns (see Table 1). This distribution is typical for all considered computations. It clearly shows the predominance in the CPU costs of the multigrid scheme which behaves like $O(n)$.

4.2. Isospectral geometries

By asking "can one hear hear the shape of a drum?", Kac [25] referred to the question whether the Laplacian operator with Dirichlet boundary conditions could have identical spectra on two different planar regions. A counterexample proposed by Gordon et al. [14], the so-called GWW isospectral drum, answered the question negatively. It is well known that the computation of the spectrum of these isospectral drums is numerically so involved (see the survey [12]) that the determination of the higher eigenpairs has been realized by means of experiments based on microwave devices [40]. Clearly, isospectral geometries and especially the GWW drums (see Fig. 3) offer a challenging and ideal set-up to validate our approach.

The computed spectrum is validated by means of two different approaches. Firstly, the computed spectra of both the GWW drums (see Fig. 3) are compared (see Fig. 4). One can clearly derive from these results the isospectral property of both drum geometries. Secondly, the numbers of computed eigenvalues less than λ denoted by $\tilde{N}(\lambda)$ are compared with the exact number of eigenvalue $N(\lambda)$ less than λ approximated by the corrected Weyl formula for polygons which is [5]

$$N(\lambda) \approx \frac{A}{4\pi}\lambda - \frac{P}{4\pi}\sqrt{\lambda} + \sum_{i=1}^{N} \frac{1}{24}\left(\frac{\pi}{\alpha_i} - \frac{\alpha_i}{\pi}\right), \tag{4.22}$$

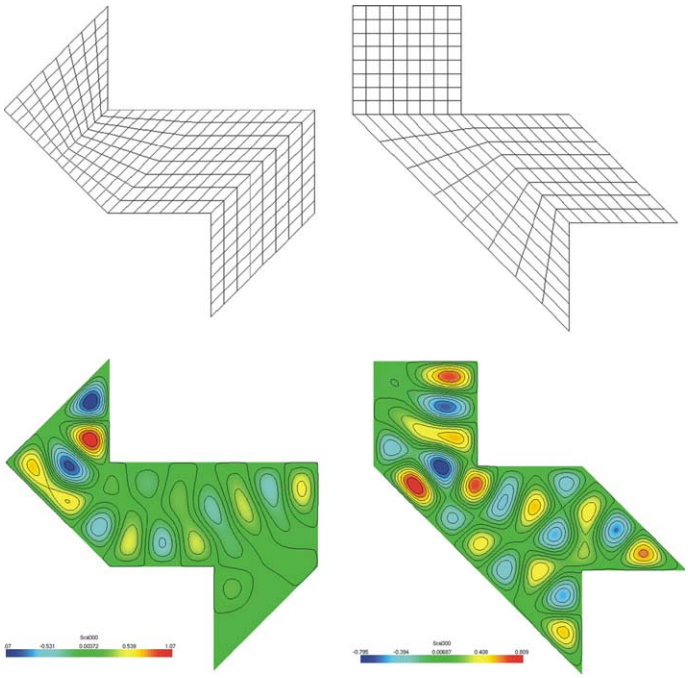

Fig. 3. Third refinement grid of the GWW isospectral drums (upper row), and corresponding 30th eigenfunctions (lower row) computed on the sixth refinement level (~20,0000 unknowns) considering the method described in [24].

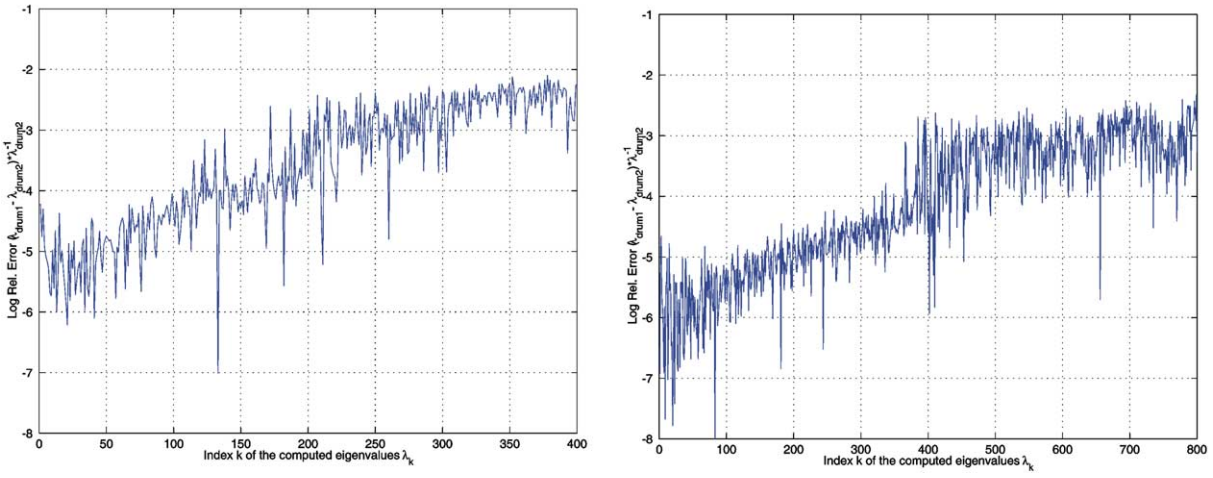

Fig. 4. Relative error obtained by comparing with each other the spectra of both drums defined in Fig. 3 on the sixth refinement level (~60,000 unknowns) (left) and on the seventh refinement level (~20,0000 unknowns) (right).

where A (resp. P) denotes the area (resp. perimeter) of Ω, N the number of corners and α_j are the interior angles at the vertices of Ω such that $0 < \alpha_i < 2\pi$ for $i \in [1, N]$. The corresponding results for the drum on the right-hand side of Fig. 3 are presented in Fig. 5. Similar results are obtained for the second drum geometry.

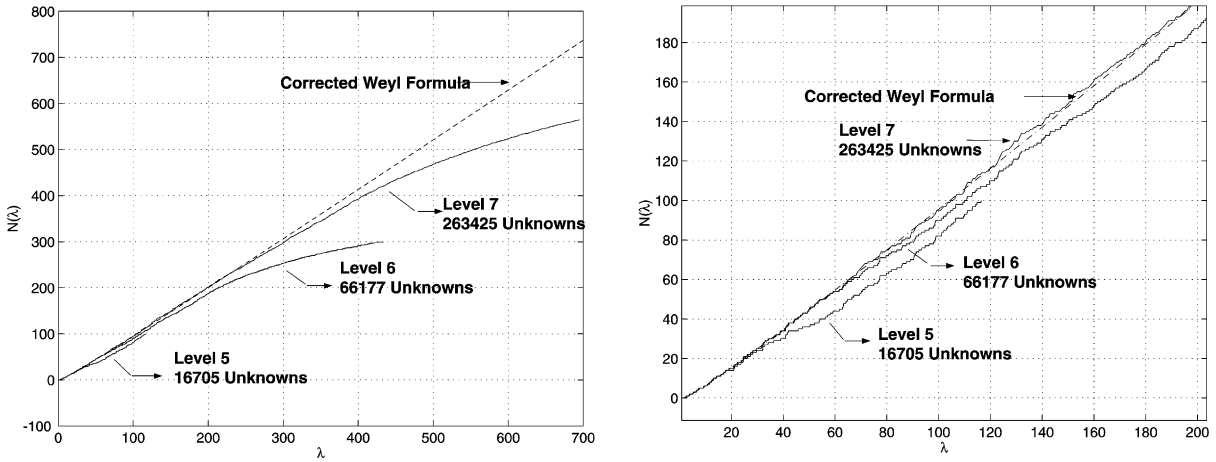

Fig. 5. Integrated eigenvalue density for the GWW drums. The dashed line represents the corrected Weyl's formula (4.22) and the solid line the computed number of eigenvalues $\tilde{N}(\lambda)$ below λ on the respective refinement levels. A zoom of the left curves in the range $\lambda \in [0, 200]$ is presented on the right.

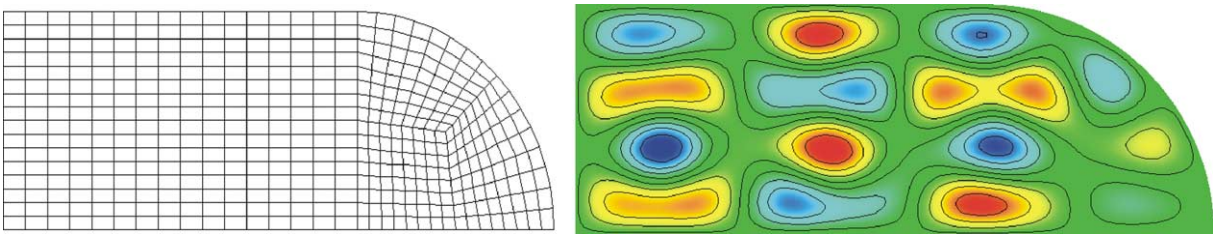

Fig. 6. Third refinement grid of the Bunimovich stadium $\gamma = 1.8$ and corresponding 30th eigenfunction computed on the sixth refinement level (~12,0000 Unknowns) by means of the method descried in [24].

4.3. Bunimovich stadium

The so-called Bunimovich stadium (a quarter of which is depicted in Fig. 6) belongs to the class of billiard geometries which has been widely investigated both theoretically and experimentally (see e.g. [34] and reference therein). In the classical limit this model billiard is known to be fully chaotic. The properties of the associated quantum billiard have been extensively studied experimentally through the construction of electromagnetic cavities.

The goal of this section is to validate the proposed numerical approach through comparisons with experimental data. We restrict these comparisons to the results presented in [1,15,34]. We assume a Bunimovich stadium with radius $r = 0.2\,\mathrm{m}$ and length $l = 0.36\,\mathrm{m}$ corresponding to $\gamma = l/r = 1.8$. We consider further a statistical analysis of the computed eigenvalue sequence based on the nearest neighbor spacing distribution (NND) given in form of an histogram in Fig. 7. For a given sequence of eigenvalues $\{\lambda_1, \ldots, \lambda_m\}$ one compute the spacings $s_i := (\lambda_{i+1} - \lambda_i)/\bar{s}$, whereas $\bar{s}$ is the average distance of the computed eigenvalues. The proper normalization of the obtained spacings yields then the spacing distribution denoted $P(s)$ in Fig. 7 (see [35] for more details).

The obtained distribution on the finest grid is in very good agreement with the experimental results presented in [1,34]. It coincides with the Gaussian Orthogonal Ensemble (GOE) distribution. The deviation of the

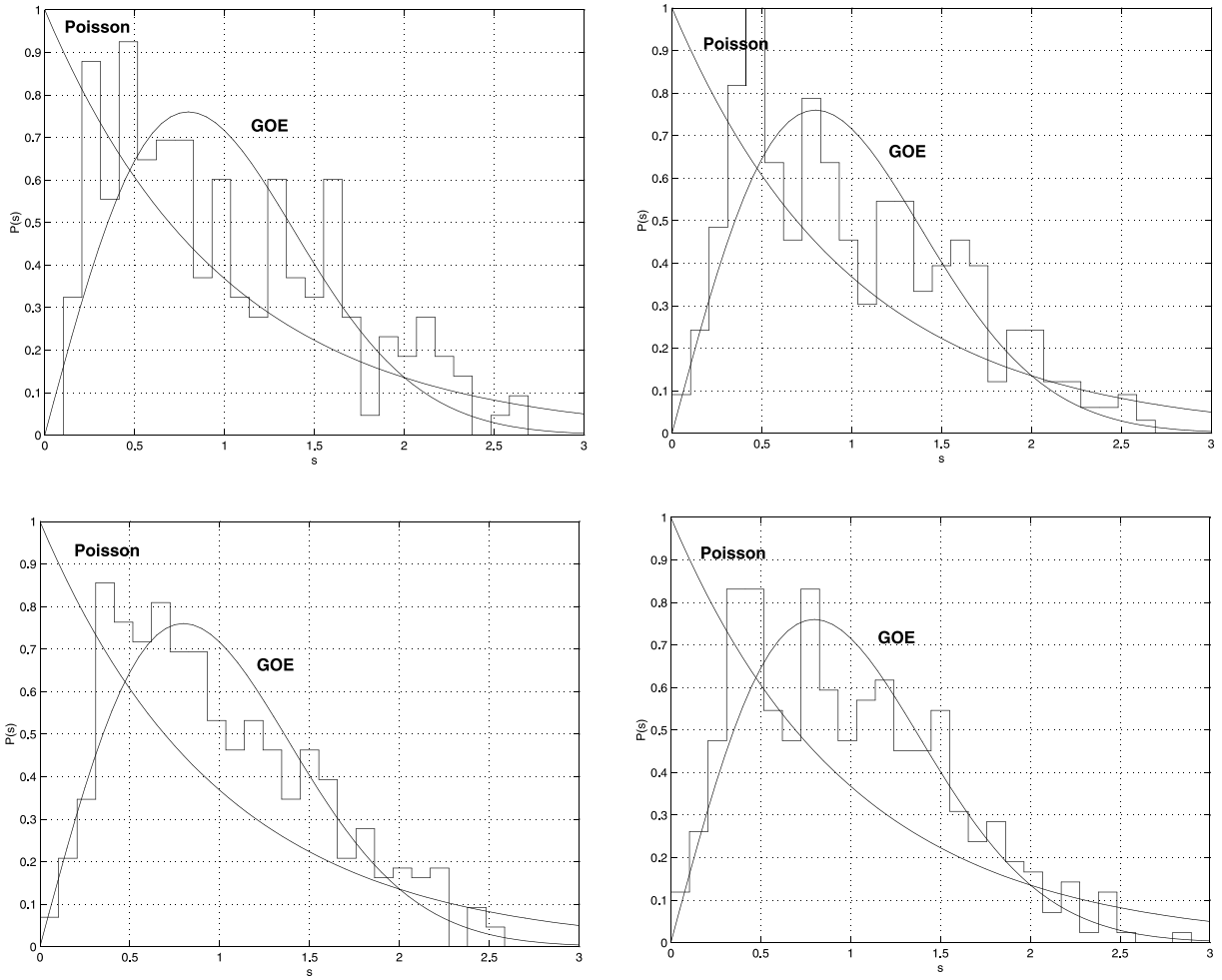

Fig. 7. Nearest neighbor spacing distribution (NND) in the quarter of the Bunimovich billiard $\gamma = 1.8$ (see Fig. 6) is represented by the histogram and is compared to the Poisson and GOE distribution for the following refinement level: level 5/28993 unknowns (up/left), level 6/115329 unknowns (up/right), level 7/460033 unknowns (down/left), and level 8/1.8 million unknowns (down/right).

Table 4
Number of valid eigenvalues considering condition (4.23) and corresponding maximal resolved frequency in the sense of expression (4.20) on the grid hierarchy for a Q_2 discretization

Refinement level	4	5	6	7	8
# Unknowns	7329	28993	115329	460033	1.8 million
# Validated eigenvalues	38	234	435	665	927
Maximal frequency (GHz)	4.1	6 .2	9.3	11.2	14.1

GOE distribution also observed experimentally is discussed in [34]. In Table 4, we show the maximal frequency in the sense of Eq. (4.20) which can be accurately resolved on the considered discretization level. The validity of the computed eigenvalues checked by means of the following approximation of the Weyl formula:

$$N(\lambda) \approx \frac{A}{4\pi}\lambda - \frac{P}{4\pi}\sqrt{\lambda},$$

where A denotes the area of the billiard and P its perimeter. A sequence of eigenfrequencies is considered to be valid if the number of computed eigenvalues less than a λ denoted by $\tilde{N}(\lambda)$ fulfills following condition:

$$|N(\lambda) - \tilde{N}(\lambda)| \leqslant 5. \tag{4.23}$$

5. Conclusion

In this paper, we propose a new method for the computation of a large number of eigenvalues of selfadjoint elliptic operators which is based on the interplay of the Lanczos tridiagonalization scheme and multigrid techniques for linear systems. The resulting scheme requires $O(mn)$ arithmetic operations and $O(n)$ memory capacity, where n is the number of unknowns and m the number of needed eigenvalues. The numerical experiments which focus on the numerical simulation of chaos manifestation in quantum mechanics, clearly validate the proposed approach which opens new perspectives in that context. It allows indeed to consider complex geometries (containing for example holes) for which the experimental realization may be delicate if possible at all. Furthermore, the systematic study of the transition from integrable to non-integrable classical chaotic behavior on successively deformed geometries may be tackled numerically. These aspects as well as the embedding of the proposed approach on parallel platforms will be the object of a forthcoming paper.

Acknowledgements

The author acknowledges Rolf Rannacher for many fruitfull discussions as well as valuable comments. This work was supported by the SFB 359 'Reaktive Strömungen, Diffusion und Transport'.

References

[1] H. Alt, C. Dembowski, H.-D. Gräf, R. Hofferbert, H. Rehfeld, A. Richter, C. Schmit, Experimental versus numerical eigenvalues of a Bunimovich stadium billiard: a comparison, Phys. Rev. E 60 (3) (1999).
[2] E. Anderson, Z. Bai, C. Bischof, S. Blackford, J. Demmel, J. Dongarra, J. Du Croz, A. Greenbaum, S. Hammerling, A. McKenney, D. Sorensen, LAPACK Users' Guide, third ed., SIAM, 1999.
[3] I. Babuška, H.C. Elman, K. Markley, Parallel implementation of the *hp*-version of the finite element method on a shared-memory architecture, SIAM J. Sci. Stat. Comp. 13 (1992) 1433–1459.
[4] I. Babuska, J.E. Osborn, Eigenvalue problems, in: P.G. Ciarlet, J.L. Lions (Eds.), Handbook of Numerical Analysis, Volume 2, Chapter Finite Element Methods (Part 1), Elsevier, The Netherlands, 1991, pp. 641–792.
[5] H.P. Baltes, E.R. Hilf, Spectra of finite systems. Bibliographisches Institut Mannheim, Wien, Zurich, 1976.
[6] H. Blum, Q. Lin, R. Rannacher, Asymptotic error expansion and Richardson extrapolation for linear finite elements, Numer. Math. 49 (1986) 11–37.
[7] J.H. Bramble, J.E. Osborn, Rate of convergence estimates for non-selfadjoint eigenvalue approximations, Math. Comp. 27 (123) (1973) 525–549.
[8] P.G. Ciarlet, The Finite Element Method for Elliptic Problems, North-Holland, Amsterdam, 1987.
[9] R. Courant, D. Hilbert, Methoden der mathematischen Physik, Springer, Berlin, 1968.
[10] J. Cullum, R.A. Willoughby, The Lanczos phenomenon – an interpretation based upon conjugate gradient optimization, Linear Algebr. Appl. 29 (1980) 63–90.
[11] J. Cullum, R.A. Willoughby, Computing eigenvalues of very large symmetric matrices – an implementation of a Lanczos algorithm with no reorthogonalization, J. Comp. Phys. 44 (1981) 329–358.

[12] T.A. Driscoll, Eigenmodes of isospectral drums, SIAM Rev. 39 (1) (1997) 1–17.
[13] T. Ericsson, A. Ruhe, The spectral transformation Lanczos method for the numerical solution of large sparse generalized symmetric eigenvalue problems, Math. Comp. 35 (152) (1980) 1251–1268.
[14] C. Gordon, D. Webb, S. Wolpert, Isospectral plane domains and surfaces via riemannian orbifolds, Invent. Math. 110 (1992) 1–22.
[15] H.-D. Gräf, H.L. Harney, H. Lengeler, C.H. Lewenkopf, C. Rangachryulu, A. Richter, P. Schardt, H.A. Weidenmüller, Distribution of eigenmodes in a superconducting stadium billiard with chaotic dynamics, Phys. Rev. Lett. 69 (9) (1992) 1296–1299.
[16] A. Greenbaum, Z. Strakos, Predicting the behavior of finite precision Lanczos and conjugate gradient computations, SIAM J. Matrix Anal. Appl. 13 (1) (1992) 121–137.
[17] T. Guhr, A. Müller-Groeding, H. Weidenmüller, Random matrix theories in quantum physics: common concepts, Phys. Rep. 299 (1998).
[18] M.C. Gutzwiller, Periodic orbits and classical quantization conditions, J. Math. Phys. 12 (1971) 343–358.
[19] M.C. Gutzwiller, Chaos in Classical and Quantum Mechanics Interdisciplinary Applied Mathematics, Springer, Berlin, 1990.
[20] W. Hackbusch, Multi-grid Methods and Applications, Springer, Berlin, 1985.
[21] W. Hackbusch, Elliptic Differential Equations, Springer, Berlin, 1992.
[22] W. Hackbusch, Integral equations: Theory and Numerical Treatment volume 120 of International Series of Numerical Mathematics, Birkhäuser, Basel, Switzerland, 1995.
[23] V. Heuveline, HiFlow, a C++ *hp*-Finite Element toolbox for numerical simulation of PDEs. Available from. http://www.hiflow.de, 2001.
[24] V. Heuveline, C. Bertsch, On multigrid methods for the eigenvalue computation of non-selfadjoint elliptic operators, East-West J. Numer. Math. 8 (2000) 275–297.
[25] M. Kac, Can one hear the shape of a drum?, Am. Math. Mont. 73 (4) (1966) 1–23.
[26] A.V. Knyazev, K. Neymeyr, Efficient solution of symmetric eigenvalue problems using multigrid preconditioners in the locally optimal block conjugate gradient method, Technical Report 163, University of Tübingen and Stuttgart, July 2001.
[27] C. Lanczos, An iteration method for the solution of the eigenvalue problem of linear differential and integral operators, J. Res. Natl. Bureau Stand. 45 (1950) 255–282.
[28] K. Meerbergen, The rational Lanczos method for Hermitian eigenvalue probelms, Numer. Linear Algebr. Appl. 8 (2001) 33–52.
[29] J.M. Melenk, K. Gerdes, C. Schwab, Fully discrete *hp*-finite elements: Fast quadrature, Technical Report 1999-15, Seminar for Applied Mathematics, ETH Zurich, 1999.
[30] B. Nour-Omid, B.N. Parlett, T. Ericsson, P.S. Jensen, How to implement the spectral transformation, Math. Comp. 48 (178) (1987) 663–673.
[31] J.E. Osborn, Spectral approximation for compact operators, Math. Comp. 29 (13) (1975) 712–725.
[32] C.C. Paige, Computational variants of the Lanczos method for the eigenproblem, J. Inst. Math. Appl. 10 (1972) 373–381.
[33] B.N. Parlett, The Symmetric Eigenvalue Problem, Prentice Hall, Englewood Cliffs, NJ, 1980.
[34] A. Richter, Playing billiards with microwaves – Quantum manifestations of classical chaos, in: Emerging Applications of Number Theory, Volume 109 of The IMA Volumes in Mathematics and its Applications, Springer, New-York, 1998, pp. 479–523.
[35] A. Richter, Test of trace formulas for spectra of superconducting microwave billiard, Found. Phys. 31 (2001).
[36] A. Ruhe, Rational krylov sequence methods for eigenvalue computation, Linear Alg. Appl. 58 (1980) 391–405.
[37] Y. Saad, Numerical Methods for Large Eigenvalue Problems, Halstead Press, New York, 1992.
[38] Y. Saad, Iterative methods for sparse linear systems, Computer Science/Numerical Methods, PWS Publishing Company, 1996.
[39] C. Schwab, *p*- and *hp*-Finite Element Methods, Theory and Applications in Solid an Fluid Mechanics. Numerical Mathematics and Scientific Computation, Oxford University Press, Oxford, 1998.
[40] S. Sridhar, A. Krudolli, Experiments on not "hearing the shape" of drums, Phys. Rev. Lett. 72 (1994) 2175–2178.
[41] G. Strang, G.J. Fix, An Analysis of the Finite Element Method. Automatic Computation, Prentice-Hall, Englewood Cliffs, NJ, 1973.
[42] U. Trottenberg, C. Oosterlee, A. Schüller, Multigrid, Academic Press, New York, 2001.
[43] P. Wesseling, An Introduction to Multigrid Methods, Wiley, New York, 1991.
[44] K. Yosida, Functional Analysis, sixth ed., Springer, Berlin, 1980.